



Fermi National Accelerator Laboratory  
Technical Division  
Development and Test Department  
Mail stop 316  
P.O. Box 500  
Batavia, Illinois • 60510

TD-03-017  
4/29/2003

## 2D MECHANICAL ANALYSIS OF THE STRAIGHT SECTION OF HFDB-03 “*RACETRACK* #3”

G. Ambrosio, N. Andreev, P. Bauer, S. Bhashyam

### *Abstract:*

*In the R&D effort toward a post-LHC hadron collider, Fermilab is developing a 10-12 T block-type, common-coil dipole magnet operating at 4.5 K using Nb<sub>3</sub>Sn superconductor with the React-and-Wind technology. As part of the development of the React-and-Wind technology, flat racetrack coils have been tested in the so-called “Racetrack magnet” [1]. This note reports the finite element (FE) analysis of the cross-section of the straight section of HFDB-03 (Racetrack #3). The mechanical design of HFDB-03 is similar to the one of HFDB-02, and the FE model used in this analysis is the one used for HFDB-02 [2] with a few modifications described in the following. Results are presented after pre-stress application, cooldown and under the maximum magnetic forces. A complementary analysis may be found in [3] where a 2D analysis is performed on the plane of the winding. The results of these analyses have been used to set the pre-load applied during the fabrication of HFDB-03 [4].*

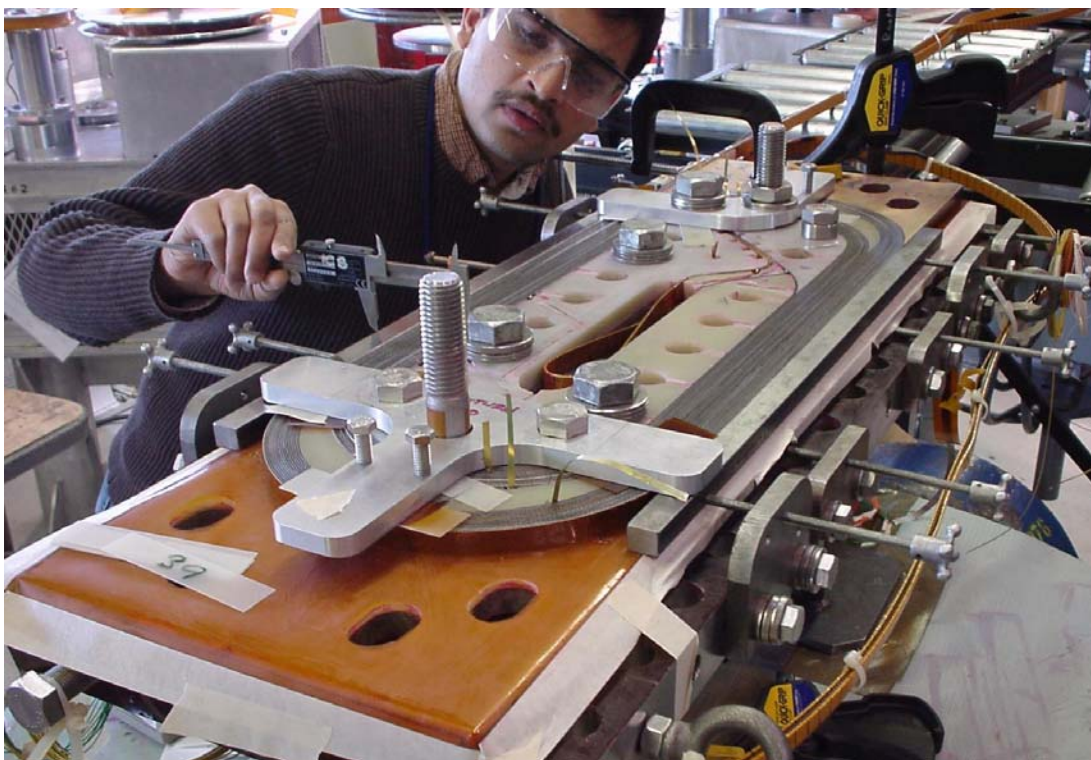


Fig. 1: HFDB-03 after winding the top coil. The end-shoes have been installed in the lead end, not yet in the return end. The turn-to-turn insulation is visible on the outer face of the last turn

## 1. RACETRACK DESIGN

HFDB-03 consists of two flat racetrack coils (Fig. 1), wound using a pre-reacted  $\text{Nb}_3\text{Sn}$  cable and connected by a  $\text{NbTi}$  cable. It is the third in a series of Racetrack magnets [1] designed to achieve a field of 10-11 tesla at 4.5 K. The goal is to study the behavior of coils fabricated with the React-and-Wind technology and to compare the critical current degradation in these magnets with the degradation measured on short samples of wires and cables. The Racetrack magnets contain no iron because a simple mechanical structure was preferred to a larger and more complicated structure, which would allow iron in close proximity to the coils (iron outside the mechanical structure would have a very low efficiency). They use a 41-strand cable made of 0.7 mm diameter wires. The bending radius in the ends is 90 mm.

The coils of HFDB-03 have 28 turns. The maximum field in HFDB-03 coils (10 T) is in the center (i.e. fourteenth and fifteenth turn) of the straight section (Fig. 5).

The main components of the mechanical structure are two 40 mm thick stainless steel plates (“main plates” in the following, indicated by A in Figure 2), which provide pre-stress and support of the main component of the magnetic force (in the direction normal to the coil plane). 57 stainless steel bolts, with a 25 mm diameter, (pre-loaded at 2300-1000 kg after magnet impregnation) should restrain the coil separation within 0.1 mm at maximum field. Side pushers (B) provide vertical pre-stress and support by means of 32 aluminum-alloy bolts, each with 12 mm diameter. In the ends pre-stress and support are given on each end-shoe by bullets (8 per end) threaded to a 44 mm-thick end plate (C). Eight bolts, with a 20 mm diameter, connect those plates to the main plates. All plates, pushers and bolts (except those in

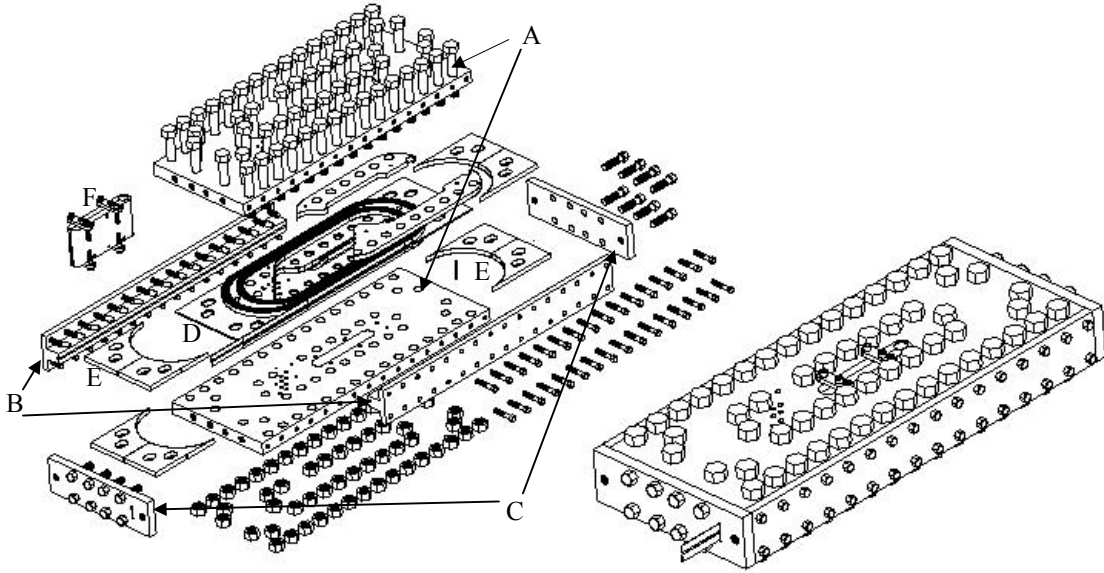


Fig. 2: Racetrack assembly, see text for details. The end plates (C) are an old design without bullets and less thick than present plates.

the sides) are made of non-magnetic stainless steel. A 5 mm-thick G10 plate (D) separates the coils. End-shoes (E) are made of brass. All parts inside the coils, both in the ends and in the straight section, are made of G10. The NbTi cable connecting the coils is pre-shaped around a G10 rod and closed inside a G10 block (F). Pins are used to center the coil inserts and the inter-coil plate to the bottom main plate.

After assembly the magnet was vacuum impregnated with epoxy. After impregnation the external surface of the magnet was cleaned of epoxy, the side pushers, the end plates and all bolts were extracted, cleaned, re-inserted and pre-stress was applied.

A more detailed description of the Racetrack magnet design can be found in [1]. The fabrication procedure of HFDB-03 is reported in [4].

## 2. LORENTZ FORCE CALCULATION

The magnetic forces in the straight section of HFDB-03 were calculated by ANSYS<sup>®</sup> at 17 kA. HFDB-03 short sample limit at 4.2 K is 16.5 kA including the bending degradation [4]. The magnetic field intensity at 17 kA in the coil and surrounding parts is shown in Fig. 5. The peak field at 17 kA is 10.2 T. The direction of the magnetic force in the coil cross-section is shown in Figure 6.

Force	(kN/m)
Horizontal	1531
Vertical	0.3

Table 1: Total Lorentz-force in the straight section of HFDB-03 at 17 kA.

### 3. FINITE ELEMENT MODEL OF THE CROSS-SECTION

The finite element (FE) model used for this analysis is a modification of the one used for the analysis of the first Nb<sub>3</sub>Sn racetrack magnets built at Fermilab (HFDB-01 and 02). The description of that model may be found in [2]. Here we report the modifications introduced to the original model.

- The mesh density of the G10 island and the stainless steel pusher was increased in some areas close to the coil
- The mesh density was also increased on the left and right side of the G10 shim (see Figures 3 and 4); contact elements were set between the G10 shim and the ground insulation (reducing the stress concentration previously visible on the top right corner of the coil)
- Contact was removed between the side pusher and the part of the ground insulation that models the quench heater
- The thickness of the stainless steel slabs, modeling the bolts, was slightly reduced in order to model only the straight section of the magnet
- It was made possible to apply a different pre-load to the horizontal bolts outside the coil (upper bolts in Fig. 3) with respect to those inside the coil (lower bolts in Fig. 3)
- The height of the protrusion on the top of the stainless steel pusher was extended to 9 mm in order to simulate the use of two stainless steel washers on the aluminum bolts.

The geometrical parameters used for this model are reported in Table 2. The thickness of ground insulation in the model corresponds to the thickness of the ground insulation and the quench heater in the magnet. The model used to study HFDB-01 and 02 had an option to undersize the ground insulation where it faces the stainless steel pusher. In [2] results with this option both ON and OFF were presented. During the fabrication of HFDB-03 the side pushers were cleaned after impregnation removing the layer of epoxy between them and the ground insulation on the main plates. The thickness of this layer was approximately equivalent to the thickness of the quench heater (0.3 mm). Therefore this option was used in all the analyses here presented, in order to have a 0.3 mm gap (see Fig. 4) between the side pusher and the ground insulation on the main plate.

Item	(mm)
Height of steel plate	182.5
Width of steel plate	40
Height of coil	42.08
Width of coil	15.25
Height of G10 island	90
Width of G10 island	15.25
Height of top shim	3
Width of top shim	15.25
Pusher width max	57.8
Pusher width min	17.75
Pusher height max	66.72
Pusher height min	19.05
Ground insulation width	0.89
G10 plate width	2.5
G10 plate height	139.7
Horizontal bolt equivalent thickness	8.4
Vertical bolt equivalent thickness	2.1

Table 2: Geometrical parameters of HFDB-03 model (values refer to one “quadrant”).

## 4. MATERIAL PROPERTIES

Table 3 lists the material properties used in the FE calculations presented in this note. The transverse modulus of the coil (Y direction in Table 3) was measured, at room temperature, on samples extracted from HFDB-02 [3]. The turn-to turn insulation of HFDB-03 was the same of HFDB-02: two tapes (76  $\mu\text{m}$  Kapton and 160  $\mu\text{m}$  pre-preg) wound together with the coil [5]. The value in X-direction was obtained scaling the transverse value by 1.3 according to [6]. The values at 4.2 K were obtained scaling those at room temperature by 1.3-1.4 based on measurement of many  $\text{Nb}_3\text{Sn}$  impregnated samples [7]. The properties of shim and coil-island are those of G10 with the clothes oriented in vertical direction. Both the coil-islands and the shims were cut from of a G10 plate, 15.25-mm thick, in order to have these properties (i.e. the highest thermal contraction in the horizontal direction). The thermal contraction coefficient used for Kapton is consistent with the thermal contraction measured on ten-stacks made of bare cables and Kapton insulated cables [7].

Magnet Component		Elasticity Modulus				Thermal Contraction Coefficient			
		300 K [GPa]		4.2 K [GPa]		300–4.2K [mm/m]		per 1 K [ $\mu\text{m}/\text{m}/\text{K}$ ]*	
		X	Y	X	Y	X	Y	X	Y
Coil	Impregn. Cu/ $\text{Nb}_3\text{Sn}$ , Kapton + prepreg ins	13	10	18.2	13	3.3	4.5	11.5	15.6
Ground Insulation	Kapton	3	3	3.8	3.8	13	13	45	45
Shim and Island	G10	14	18	14	18	7.62	2.75	26.4	9.5
Structure and bolts	Stainless Steel 316	210	210	225	225	3	3	10.3	10.3
Bolts	Aluminum	70	70	81.6	81.6	4.24	4.24	14.7	14.7

Table 3: Material Properties used in the analyses presented in this report (\*calculated from integrated contraction between 300 and 4 K, assuming a linear contraction coefficient)

## 5. RESULTS

Several analyses have been performed, under different preloads, aiming at the following:

- minimum horizontal pre-stress at room temperature, in order to have after cooldown zero pre-stress and no gap between coil and main plate,
- room temperature load on the aluminum bolts (for vertical pre-stress) similar to the one proposed in [3] for the straight section.

Table 4 summarizes the results at the end of the optimization. The bolts load, the stress on the coil (averaged on the top or right side of the coil as shown in Fig. 3) and the horizontal coil displacement are presented after pre-stressing, after cooldown and at maximum field (17 kA). For comparison the same results are presented in Table 5, in case of higher bolts load. It can be seen that the coil displacements are very similar in the two cases, showing that there is no need to have any horizontal preload after cooldown. Some horizontal preload is required at

room temperature in order to compensate for the differential thermal contraction of the coil and the stainless steel bolts. Without this minimum pre-stress a gap would open during cooldown, between the coil and the main plate.

<i>File: "rIII_mec_n5"</i>	unit	prestress	@ 4.2 K	@ 17 kA
Vertical bolt load	N	<b>2634</b>	1602	638
Upper-horizontal bolt load	N	<b>10150</b>	276	43596
Lower-horizontal bolt load	N	<b>22930</b>	0	48303
Vertical stress in the coil (average on the top surface of the coil)	MPa	-2.9	-1.75	-3.9
Horizontal stress in the coil (average on the right surface of the coil)	MPa	-6.1	0	-37.2
Horizontal coil displacement (average on the right surface of the coil)	mm	-0.011	-0.069	-0.014

Table 4: ANSYS® simulation, racetrack model 3: optimized solution. Horizontal displacements are computed with respect to the coil position before pre-stressing. Bold fonts highlight the loads that should be applied to the bolts during pre-stressing of HFDB-03.

<i>File: "rIII_mec_1"</i>	unit	Prestress	@ 4.2 K	@ 17 kA
Vertical bolt load	N	14020	13524	12094
Upper-horizontal bolt load	N	12853	3935	42919
Lower-horizontal bolt load	N	37355	3784	48993
Vertical stress in the coil (average on the top surface of the coil)	MPa	-15.3	-14.8	-16.5
Horizontal stress in the coil (average on the right surface of the coil)	MPa	-8.6	-1.9	-37.2
Horizontal coil displacement (average on the right surface of the coil)	mm	-0.012	-0.069	-0.017

Table 5: ANSYS® simulation, racetrack model 3: high pre-stress solution. Horizontal displacements are computed with respect to the coil position before pre-stressing.

Figures 7 to 21 show the results of the optimized solution at all stages of the magnet fabrication and operation (i.e. after pre-stress application, after cooldown to 4.2 K and under the highest magnetic forces at 17 kA). At each stage the following results are presented: equivalent stress in whole model, horizontal, vertical and equivalent stress and horizontal strain in the coil. The arrows in each plot represent the forces applied by the part of the model shown in the picture to the rest of the model and/or to the boundary conditions. If the directions of the arrows are reversed, they show the forces applied on the part of the model shown in the picture. In all plots the stresses are reported in MPa and the displacements (DMX) in mm.

In Fig. 7 the displacements have been magnified in order to show the deformation of the main plate and of the side pushers under the pre-load. The bending of the main plate under the pre-load produces an uneven distribution of the horizontal pre-stress in the coil (~6 MPa difference between top and bottom of the coil). However, given the low average horizontal

pre-stress, the maximum pre-stress is quite low (10 MPa). The vertical pre-stress at room temperature is more uniform and lower than the horizontal one (~3 MPa).

During cooldown the coil shrinks more than the rest of the mechanical structure in vertical direction, but the aluminum bolts force the side pusher to remain in contact with the coil. After cooldown the vertical pre-stress in the coil is slightly reduced (~2 MPa) and there is no horizontal pre-stress. Still the coil is well constrained in the mechanical structure, as may be seen by the small displacement under the highest magnetic forces (55  $\mu\text{m}$ ) as shown in Table 3. At maximum current (17 kA) the highest horizontal and vertical stresses in the coils are respectively 43 and 23 MPa. The tensile horizontal strain in the coil is negligible and the compressive horizontal strain reaches 0.2% only in a small area at the highest field.

## 6. REFERENCES

- 1) G. Ambrosio et al., "Development of a Nb<sub>3</sub>Sn Racetrack Magnet using the React and Wind Technology", Proceedings of the ICEC 2001, Madison, WI, U.S.A.
- 2) P. Bauer, G. Ambrosio, N. Andreev, S. Yadav "2D mechanical analysis of the straight section of the Nb<sub>3</sub>Sn React and Wind Racetrack models 1&2", TD-01-076
- 3) S. Bhashyam, G. Ambrosio and N. Andreev, "2D Mechanics of HFDB-03 – Straight Section and Ends" TD-03-026
- 4) G. Ambrosio, N. Andreev and S. Bhashyam, "Production report of HFDB-03 "Racetrack #3", TD-03-018
- 5) G. Ambrosio et al., "Fabrication and Test of a Racetrack Magnet Using Pre-Reacted Nb<sub>3</sub>Sn Cable", to be published in ASC 2002 proceedings, (Houston, TX).
- 6) P. Bauer and R. Conway, Fermilab Memo 3/1/2002
- 7) D. Chichilli and R. Conway, Fermilab, private communications

## APPENDIX - PLOTS

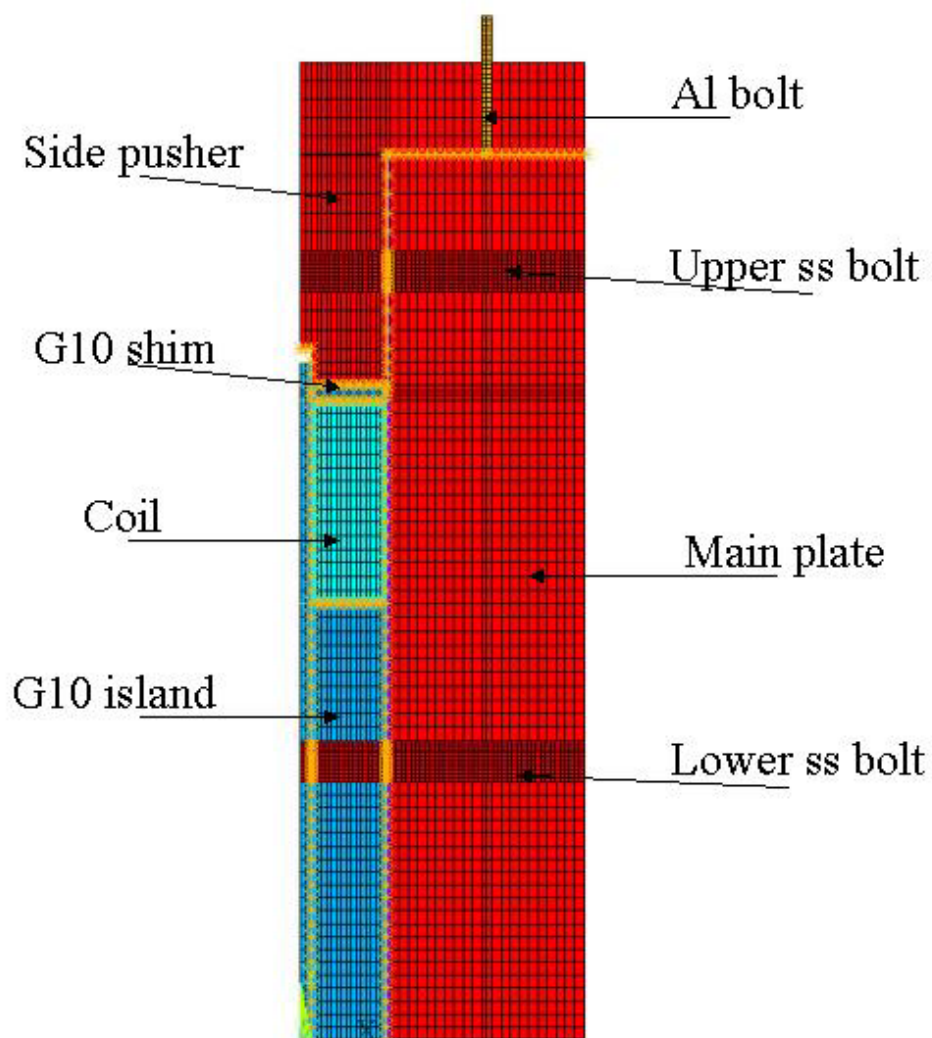


Fig. 3: Finite element model of HFDB-03 cross-section. Different colors refer to different materials. Yellow lines and asterisks show the contact elements.

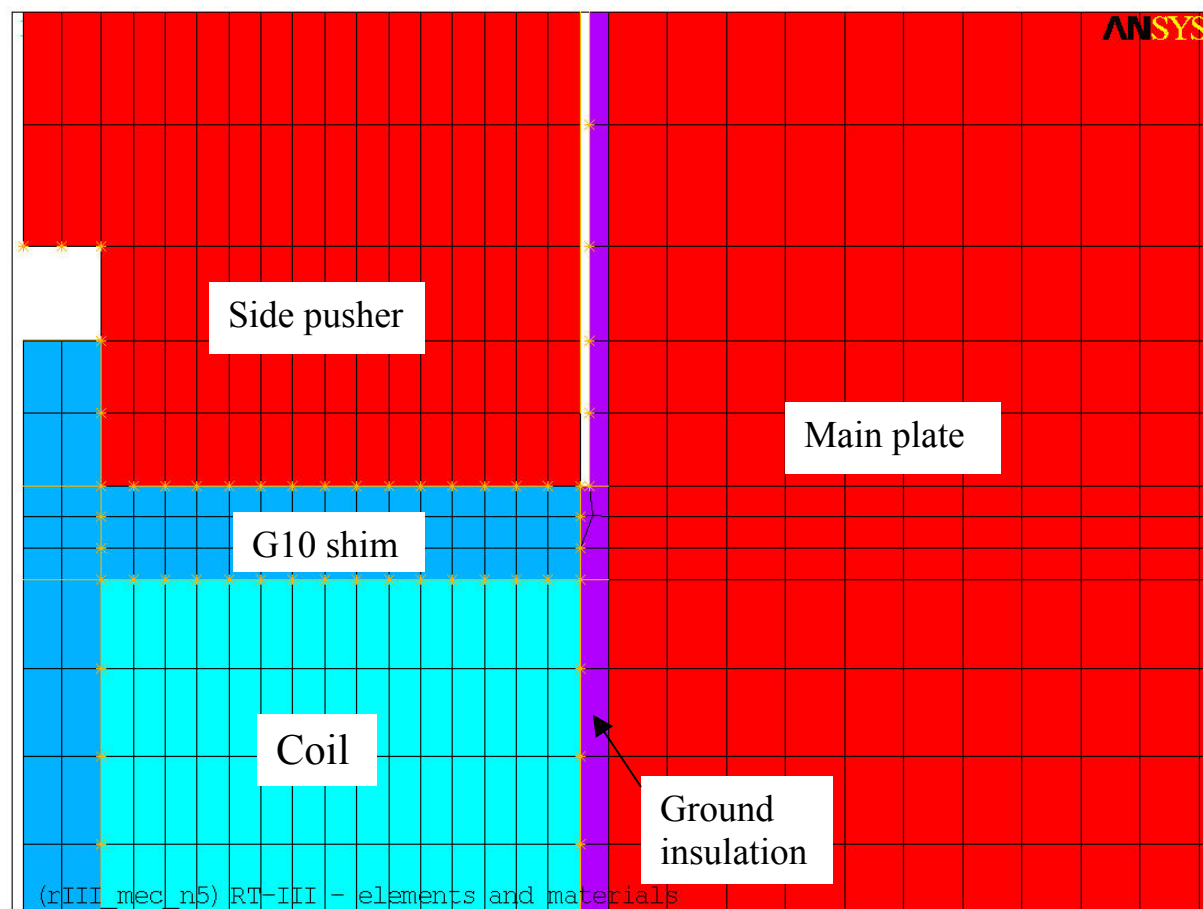


Fig. 4: Detail of the FE model showing the top of the coil, the G10 shim and the ground insulation. The gap between the side pusher and the main plate is visible in the top part of the picture. Yellow lines and asterisks show the contact elements

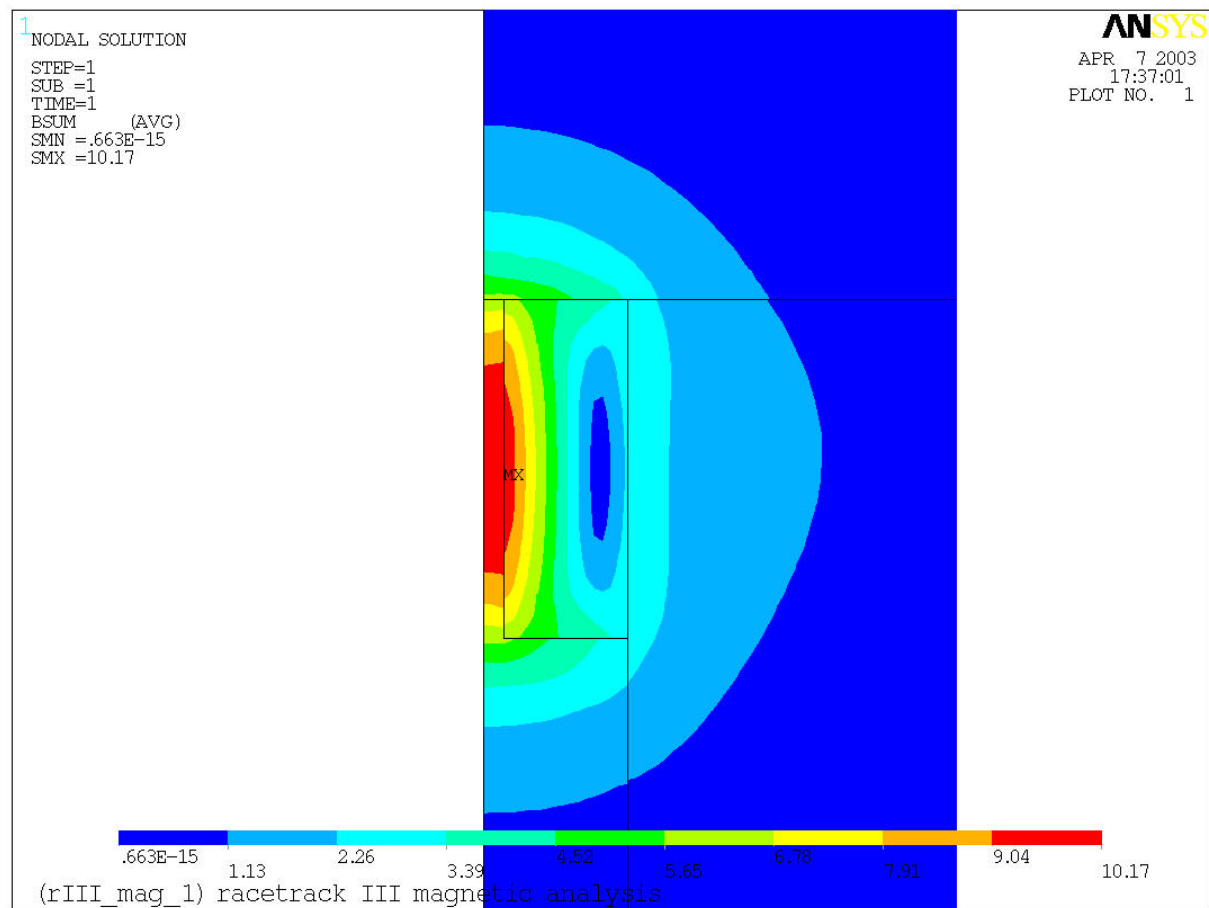


Fig. 5: Magnetic field in the coil and surrounding parts at 17 kA.

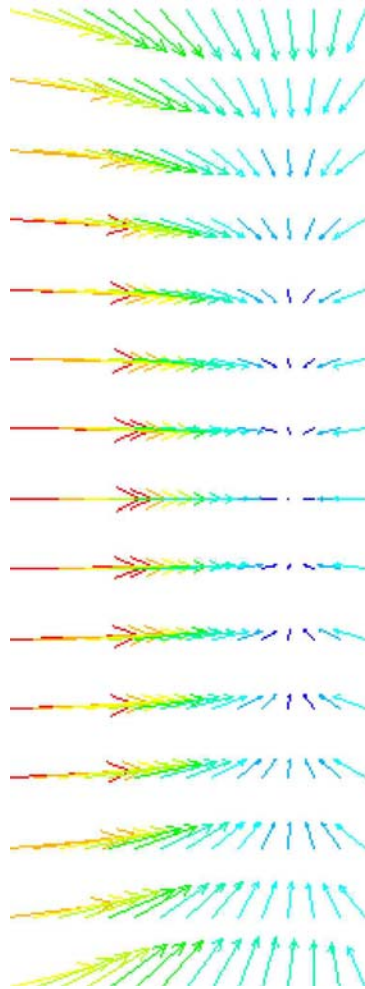
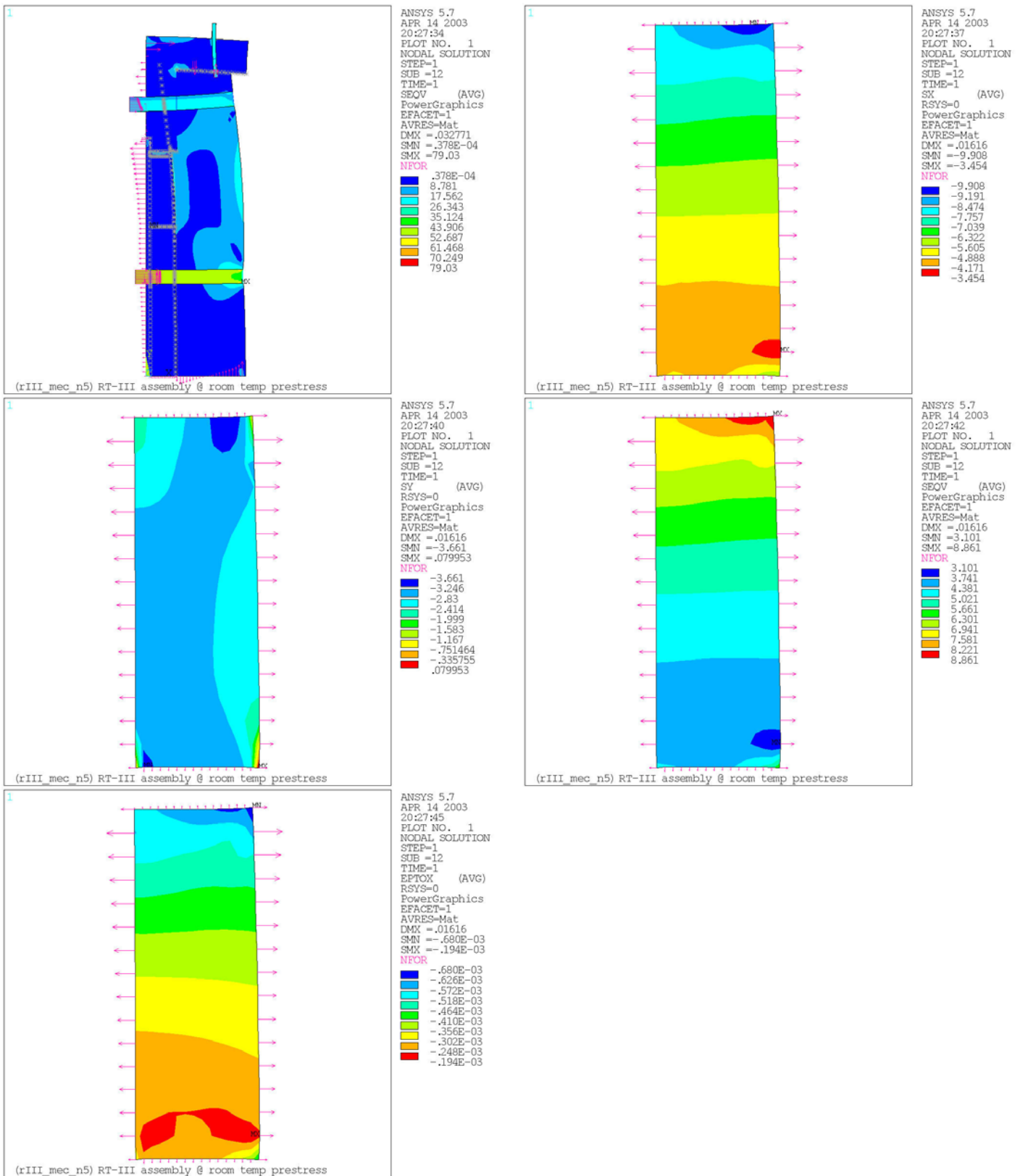
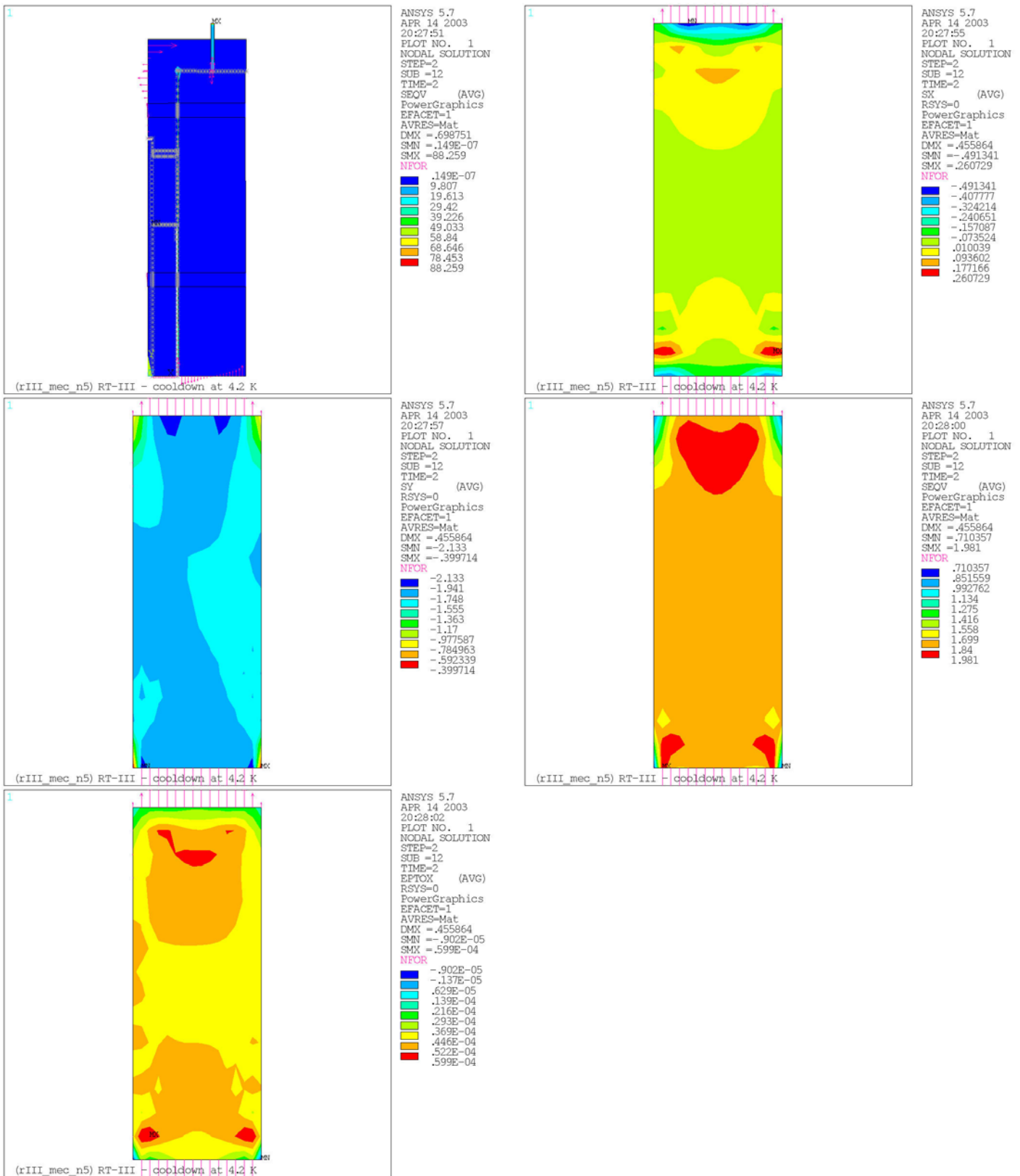


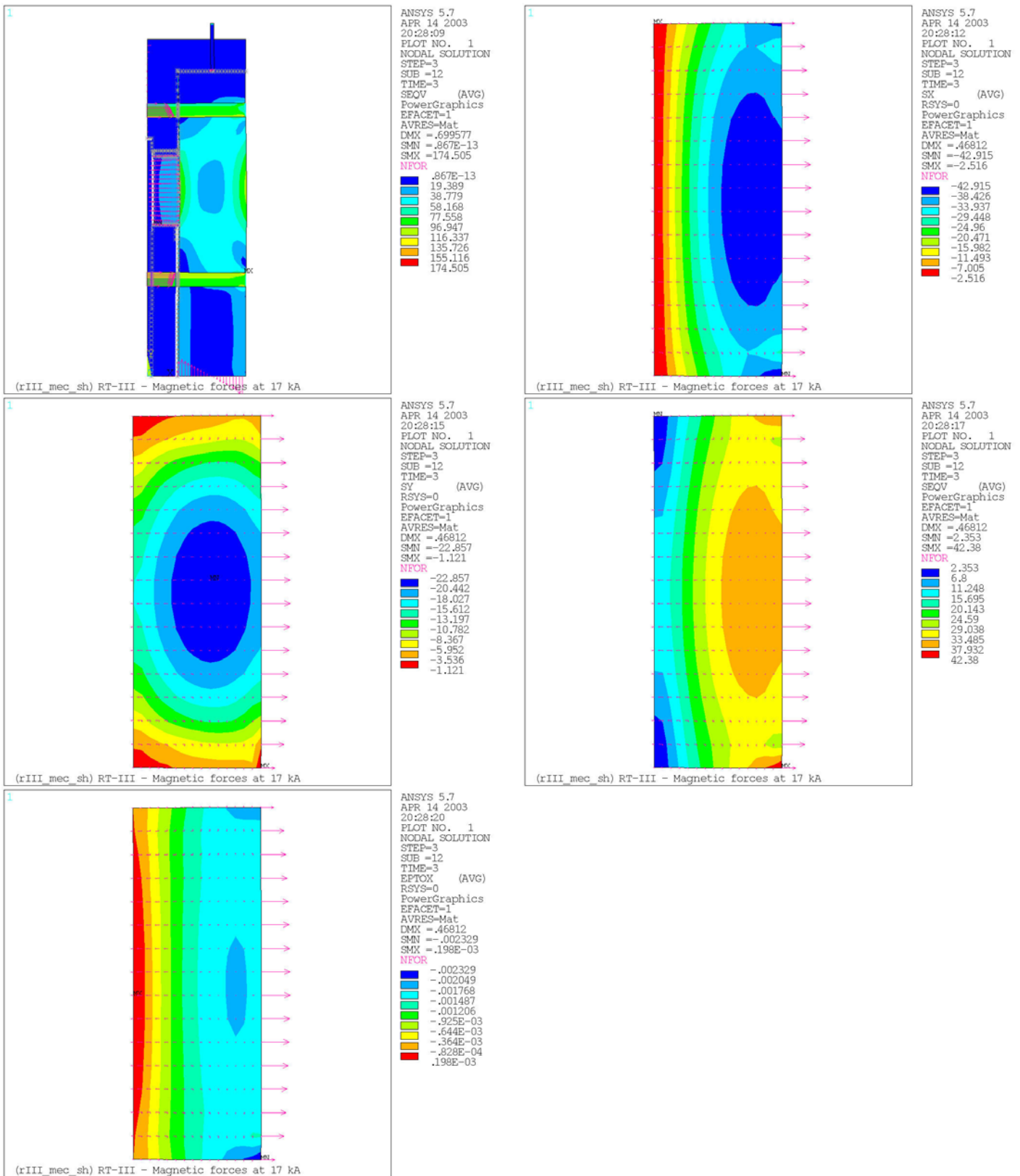
Fig. 6: Intensity (shown by color and arrow dimension) and direction of the magnetic forces in the coil.



Figures 7-11. Results after pre-stress: 7-equivalent stress in whole model, 8-horizontal stress in the coil, 9-vertical stress in the coil, 10-equivalent stress in the coil, 11-horizontal strain in the coil.



Figures 12-16. Results after cooldown at 4.2 K: 12-equivalent stress in whole model, 13-horizontal stress in the coil, 14-vertical stress in the coil, 15-equivalent stress in the coil, 16-horizontal strain in the coil.



Figures 17-21. Results at 17 kA: 17-equivalent stress in whole model, 18-horizontal stress in the coil, 19-vertical stress in the coil, 20-equivalent stress in the coil, 21-horizontal strain in the coil.